Toxicology xxx (2008) xxx–xxx

Contents lists available at ScienceDirect

Toxicology

journal homepage: www.elsevier.com/locate/toxicol

Comparative study of pulmonary responses to nano- and submicron-sized ferric oxide in rats

Mo-Tao Zhu[a,b], Wei-Yue Feng[a,*], Bing Wang[a,b], Tian-Cheng Wang[d], Yi-Qun Gu[c], Meng Wang[a,b], Yun Wang[a,b], Hong Ouyang[a], Yu-Liang Zhao[a], Zhi-Fang Chai[a]

[a] *Laboratory for Bio-Environmental Effects of Nanomaterials and Nanosafety and Key Laboratory of Nuclear Analytical Techniques, Institute of High Energy Physics, Chinese Academy of Sciences, Beijing 100049, China*
[b] *Graduate School of Chinese Academy of Sciences, Beijing 100049, China*
[c] *Hospital of Haidian District, Beijing 100080, China*
[d] *Department of Clinical Laboratory of Medicine, 3rd Hospital of Peking University, Beijing 100083, China*

ARTICLE INFO

Article history:
Received 11 January 2008
Received in revised form 18 February 2008
Accepted 18 February 2008
Available online xxx

Keywords:
Ferric oxide nanoparticle
Pulmonary response
Coagulatory disturbance
Intratracheal instillation

ABSTRACT

Ferric oxide (Fe_2O_3) nanoparticles are of considerable interest for application in nanotechnology related fields. However, as iron being a highly redox-active transition metal, the safety of iron nanomaterials need to be further studied. In this study, the size, dose and time dependent of Fe_2O_3 nanoparticle on pulmonary and coagulation system have been studied after intratracheal instillation. The Fe_2O_3 nanoparticles with mean diameters of 22 and 280 nm, respectively, were intratracheally instilled to male Sprague Dawley rats at low (0.8 mg/kg bw) and high (20 mg/kg bw) doses. The toxic effects were monitored in the post-instilled 1, 7 and 30 days. Our results showed that the Fe_2O_3 nanoparticle exposure could induce oxidative stress in lung. Alveolar macrophage (AM) over-loading of phagocytosed nanoparticle by high dose treatment had occurred, while the non-phagocytosed particles were found entering into alveolar epithelial in day 1 after exposure. Several inflammatory reactions including inflammatory and immune cells increase, clinical pathological changes: follicular hyperplasia, protein effusion, pulmonary capillary vessel hyperaemia and alveolar lipoproteinosis in lung were observed. The sustain burden of particles in AM and epithelium cells has caused lung emphysema and pro-sign of lung fibrosis. At the post-instilled day 30, the typical coagulation parameters, prothrombin time (PT) and activated partial thromboplastin time (APTT) in blood of low dose 22 nm-Fe_2O_3 treated rats were significantly longer than the controls. We concluded that both of the two-sized Fe_2O_3 particle intratracheal exposure could induce lung injury. Comparing with the submicron-sized Fe_2O_3 particle, the nano-sized Fe_2O_3 particle may increase microvascular permeability and cell lysis in lung epitheliums and disturb blood coagulation parameters significantly.

1. Introduction

Engineered nanoparticles can result in unique electronic, photonic and catalytic properties which display great differences from their bulk ones of the same materials. The highly biological and environmental activity and catalysis of nanoparticles have been widely and considerably used in disease treatment, pollutant degradation and so forth (Hanes et al., 1997; Hubbell and Langer, 1995; Torres-Martínez et al., 2001). However, such activities of nanoparticles in organisms might produce extremely high and long-term toxicity. A large amount of epidemiological and experimental studies indicate that ultrafine particles have close association with many respiratory and cardiovascular diseases, such as pneumonia, lung cancer, arteriosclerosis and myocardial infarction (Gamble and Lewis, 1996; Atkinson et al., 1999; Pope et al., 1995; Oberdörster et al., 2005). Particles in the nano-sized range have large specific surface area and high biological activity that may affect great epithelial surface area in lung and are thus more likely to deposit in the lower airways and the alveolar region (Donaldson et al., 1998). Increasing evidence demonstrated that nanoparticles could easily transfer through cell membrane, escape from macrophage phagocytosis and enter into lung interstitial (Renwick et al., 2001; Hoet et al., 2004). It is hypothesized that nanoparticles because of their long retention in the host tissues might repeat their highly catalytic activity with the host in cascade (Limbach et al., 2007).

Iron nanomaterials because of their super-paramagnetic characteristics and high catalytic abilities are of considerable interest for application in nanotechnology related fields including environmental catalysis, magnetic storage, biomedical imaging, magnetic target drug delivering, etc. (Hood, 2004). However, as a transition metal, iron is considered to play a pivotal role in modulating

* Corresponding author.
E-mail address: fengwy@mail.ihep.ac.cn (W.-Y. Feng).

0300-483X/$ – see front matter © 2008 Elsevier Ireland Ltd. All rights reserved.
doi:10.1016/j.tox.2008.02.011

oxidative stress and other biological responses in particulate matter (PM), which is speculated to be the critical mechanism in eliciting the adverse effects of PM exposure. Zhou et al. (2003) reported that inhalation of iron particles in rats caused oxidative stress associating with a proinflammatory response in lung. The research of Simeonova and Luster (1995) demonstrated that iron on asbestos fibers catalyzed hydroxyl radical generation and thus stimulated TNF-α in alveolar macrophages expression. Possessing the transition metallic and nanoparticle properties, iron nanomaterials are hypothesed to display toxicity by exposure. However, up to now, the pulmonary responses of engineered iron nanomaterials by inhalation exposure *in vivo* remain to be adequately elucidated.

In this study, the nano- (22 nm) and submicron-sized (280 nm) Fe_2O_3 particles were used to test the pulmonary responses in rats by intratracheal instillation exposure. We tested the hypothesis that exposure to Fe_2O_3 nanoparticle could result in inflammatory and oxidative stress response in lung, and simultaneously might cause blood coagulation alteration.

2. Materials and methods

2.1. Fe_2O_3 particles

Two kinds of engineered, nano- and submicron-sized Fe_2O_3 particles were used in the experiments. The nano-sized Fe_2O_3 particles with a primary particle diameter of 22 nm were purchased from Haoyun Industrial and Trade Co. Ltd., Beijing, China. The submicron-sized Fe_2O_3 particles with a primary particle diameter of 280 nm were obtained from Zunye Nanomaterials Co. Ltd., Shenzhen, China. The average size of the particle was carefully determined by transmission electron microscopy (TEM, JEM 200CX) (Fig. 1). The purity of the particles was determined by ICP-AES. The crystal form of the two-sized Fe_2O_3 particles was determined by X-ray Diffraction (XRD, PANalytical's X'Pert PRO). The specific surface area was measured by BET method using a surface area analyzer (Autosorb-1 model, Quantchrome, USA). The characterizations of the two-sized Fe_2O_3 particles were shown in Table 1.

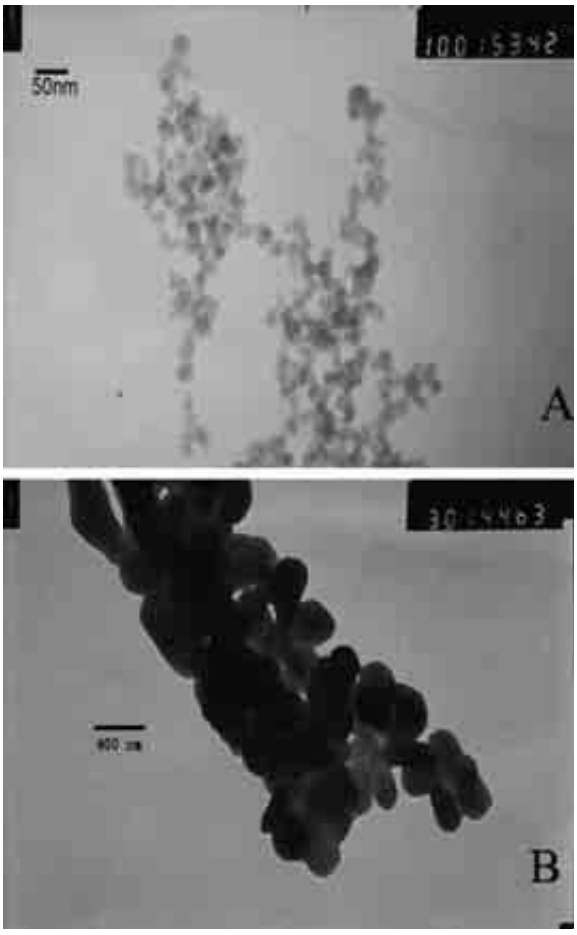

Fig. 1. (A) TEM image for 22 nm-Fe_2O_3 particles; (B) TEM image for 280 nm-Fe_2O_3 particles.

Table 1
Characterization of Fe_2O_3 particles

	Nano-Fe_2O_3	Submicron-Fe_2O_3
Particle size	22 nm	280 nm
Crystal form	Rhombohedral crystal	Rhombohedral crystal
Specific surface area	53.27 m^2/g	4.25 m^2/g
Purity	99.46%	99.77%

The particles were ultrasonic dispersed for 10 min in saline solution before every use.

2.2. Animals

Male Sprague Dawley rats weighing of 240–260 g were purchased from the Experimental Animal Center, Peking University. The animals were housed in plastic cages in a air-condition controlled room (20 ± 2 °C, 50–70% relative humidity, with a 12-h light/dark cycle). Commercial pellet diet and deionized water were available *ad libitum*. After a week acclimation, rats were divided into experimental and control groups randomly. Six rats were used in every treatment groups. All the animal studies were approved according to the Ethics Committee of Animal Care and Experimentation of the National Institute for Environmental Studies, China.

2.3. Intratracheal instillation

According to previous works of PM and nanomaterials study (Oberdörster et al., 2005; Hughes et al., 1998; Lam et al., 2004), two dosages were used in this experiment: 0.8 mg/kg bw was chosen as a low dose exposure and 20 mg/kg bw represented a high one. The animals were anesthetized by 40 mg/kg bw i.p. sodium pentobarbital (Solarbio, Germany) and then intratracheal instillation with 0.8 and 20 mg/kg bw of 22 nm- or 280 nm-Fe_2O_3 particle saline suspensions, respectively. The control group was intratracheally instilled only with saline solution instead.

2.4. Bronchoalveolar lavage (BAL)

After 1, 7 and 30 days of Fe_2O_3 particle instillation, the rats were anesthetized and immediately, 5 mL calcium and magnesium-free phosphate buffer saline (PBS) (0.1 mol/L, pH 7.3) was instilled into the lungs and lavaged for four times. The first two lavages of BAL fluid (BALF) were collected separately for biochemical assay and cell differential count. The BALF was centrifuged at 50 × *g* for 10 min at 4 °C. Free cell pellets were resuspended and the number of viable cells was recorded by a hemocytometer using the Wright's exclusion dye. The supernatant of the primary BALF was aliquoted and stored at −80 °C till use. All the BAL protocols were performed with a standard technique outlined by Gilmour et al. (2004) and Henderson (2005). The lung tissues were taken and frozen in liquid nitrogen immediately.

2.5. Biochemical and cytological analysis of BALF

The concentration of total protein in BALF supernatant was determined by a modified Bradford assay kit (Beyotime Institute of Biotechnology, Jiangsu, China) with bovine serum albumin (BSA) as the standard. The activities of lactate dehydrogenase (LDH) and acid phosphatase (ACP) in BALF were measured by colorimetric assay kits (Nanjing Jiancheng Bioengineering Institute, Jiangsu, China).

The resulting cells from the primary and the secondary lavages were combined and resuspended for cytological examination. At least 5×10^4 cells were stained with Wright's dye (Nanjing Jiancheng Bioengineering Institute, Jiangsu, China) on a glass slide. Macrophages, lymphocytes and neutrophils were counted to determine cell differentials under an oil immersion microscope with ×1000 magnification. At least 500 cells of each slide were counted.

2.6. Biochemical assay of lung homogenates

Lung tissues were homogenized in 0.1 mol/L PBS (pH 7.3) at 4 °C. The homogenate was centrifuged with 10,000 × *g* for 10 min at 4 °C and the resulting supernatant was aliquoted and stored at −80 °C.

Protein levels of lung homogenate were determined by the same method of BALF. The concentrations of total glutathione (T-GSH), reduced glutathione (GSH) and oxidized disulfide (GSSG) were measured by an enzymatic method according to the commercial assay kit procedure (Beyotime Institute of Biotechnology, Jiangsu, China). Briefly, T-GSH was assayed using the 5,5-dithio-bis (2-nitrobenzoic) acid (DTNB)-GSSG reductase recycling. GSSG was measured by measuring 5-thio-2-nitrobenzoic acid (TNB) which was produced from the reaction of reduced GSH with DTNB. The rate of TNB formation was measured at 412 nm over 3 min. The concentration of reduced GSH in the sample was obtained by subtracting GSSG from T-GSH.

Please cite this article in press as: Zhu, M.-T., et al., Comparative study of pulmonary responses to nano- and submicron-sized ferric oxide in rats, Toxicology (2008), doi:10.1016/j.tox.2008.02.011

Table 2
Percentage of macrophages, lymphocytes and neutrophils in bronchoalveolar lavage fluid (BALF) after Fe_2O_3 particle intratracheal instillation

	Post-days	Control	0.8 mg/kg bw		20 mg/kg bw	
			22 nm	280 nm	22 nm	280 nm
Macrophage %	1	89.9 ± 1.5	56.7 ± 1.7**	57.3 ± 8.3**	55.7 ± 3.0**	71.4 ± 5.9**
	7		73.5 ± 4.2**	73.7 ± 6.0**	60.6 ± 1.4**	73.2 ± 5.9**
	30		89.8 ± 2.0	87.9 ± 1.1*	82.6 ± 5.5	86.8 ± 1.7
Neutrophil %	1	6.0 ± 0.9	24.2 ± 4.8**	24.7 ± 4.3**	21.2 ± 4.3**	17.7 ± 4.2**
	7		23.8 ± 5.9*	12.7 ± 2.1**	22.9 ± 4.6**	14.0 ± 2.2**
	30		5.8 ± 1.8	7.2 ± 1.2	12.0 ± 3.3*	8.5 ± 1.4*
Lymphocyte %	1	7.2 ± 1.2	20.4 ± 6.5**	17.1 ± 12.2*	22.2 ± 5.8**	9.8 ± 1.7**
	7		6.3 ± 4.1	12.3 ± 6.0**	16.5 ± 5.2**	12.8 ± 3.7**
	30		4.6 ± 1.4	4.8 ± 1.0*	5.4 ± 2.6	4.7 ± 0.8

Data represent the mean ± S.D. (n = 6/group).
* Significant difference from control, $p < 0.05$.
** Significant difference from control, $p < 0.01$.

The lipid peroxidation product of malondialdehyde (MDA) generated in lung by free radical injury was measured by thiobarbituric acid (TBA) reactivity using the commercial colorimetric assay kit (Nanjing Jiancheng Bioengineering Institute, Jiangsu, China). The concentration of MDA was calculated by a calibration curve using 1,1,3,3′tetra-ethoxy propane as a standard and expressed as nanomole per microgram protein in tissue.

The activity of glutathione peroxidase (GSH-Px) was assayed by determination of the reduced GSH in the lung homogenate (Nanjing Jiancheng Bioengineering Institute, Jiangsu, China). Glutathione-*S*-transferase (GST) enzyme activity was measured spectrophotometrically by the standard substrate, 1-chloro-2,4-dinitrobenzene (CDNB) conjugated with GSH (Nanjing Jiancheng Bioengineering Institute, Jiangsu, China).

Nitric oxygen (NO) content in lung was measured using Griess Reagent (Beyotime Institute of Biotechnology, Jiangsu, China) by determination the concentration of $NaNO_2$ produced by NO metabolism.

2.7. Evaluation of blood coagulation

The blood samples were collected from ophthalmic veins of anesthetic rats into a 1 mL centrifuge tube with 0.1 mL of 3.8% sodium citrate pre-added. The blood plasma was separated by centrifugation at 5000 rpm for 15 min. The typical coagulation parameters, including prothrombin time (PT), activated partial thromboplastin time (APTT) and fibrinogen (FIB), were analyzed by the automated analyzer (ACL200, Beckman Coulter, USA). All the measurements had to be done within 2 h after blood collection.

2.8. Histopathological examination

After anesthesia of the rats, the non-lavaged lungs were collected and immediately immersed into 10% formaldehyde. The left piece of lung tissue was embedded into paraffin wax, then sectioned into 5 μm thick slice and mounted on a glass microscope slide using the standard histopathological techniques (Xu et al., 2003). The slices were stained with hematoxylin–eosin (HE) and examined by a light microscopy.

2.9. Transmission electron microscopy (TEM)

The non-lavaged lungs were cut into ~1 mm^3 piece and immediately fixed in 2.5% glutaraldehyde overnight, then the samples were treated according to the general protocols for TEM study. The ultra-thin sections (70–100 nm) were stained with lead citrate and uranyl acetate and the specimens were examined using JEOL JEM-100CX II electron microscopy.

2.10. Statistical analysis

For statistical analysis, all data are expressed as mean ± standard error deviation, which are shown by the bars in the graphs. A one-way analysis of variance (ANOVA) and the L.S.D. or Tamhane test is used to illustrate the significant difference between the treated groups and the control. Statistical significance is considered at $p < 0.05$.

3. Results

3.1. Biochemical and cytological assessments of BALF

In order to elucidate whether the intratracheal instillation of Fe_2O_3 nanoparticles would induce lung inflammation, the biochemical and cytological changes in BALF were analyzed in the time course after instillation. In the control group, no significant changes in the cell number or cell differentials in BALF were observed after instillation of saline (Table 2). Comparatively, a significant increase in the relative number of neutrophils, lymphocytes and macrophages in BALF was counted with a peak at day 1 post-instillation in all the Fe_2O_3 particle-treated rats ($p < 0.01$), including the 22 nm- and 280 nm-Fe_2O_3 instilled rats at doses of 0.8 and 20 mg/kg bw (Table 2).

The total protein concentration in BALF showed significant dose- and time-dependent increase. At the day 30 post-instillation, the concentrations of protein in BALF of all the particle-treated rats significantly increased by 24.4–62.7% of the controls. The 280 nm-Fe_2O_3 induced higher BALF protein content in most of the observed dose and time points than 22 nm-Fe_2O_3 did, but no statistical difference were observed between them (Fig. 2). In contrast, significant LDH release was found in the 22 nm-Fe_2O_3 instilled rat at the dose of 0.8 mg/kg bw on all the observed 1, 7, and 30 post-days ($p < 0.05$), but in 280 nm-Fe_2O_3 treated rat, LDH significant increase was only observed at day 1 post-instillation (Fig. 3). In the meantime, the activities of ACP significantly elevated at day 1 of both 22 nm- and 280 nm-Fe_2O_3 particle instillation ($p < 0.01$, Fig. 4), but no obvious changes of alkaline phosphatase (AKP) were found (data not shown here).

3.2. Oxidative stress

The activity of GSH-Px significantly increased at day 1 after 0.8 mg/kg bw of 22 nm- and 280 nm-Fe_2O_3 instillation (Fig. 5). As for the high dose of 20 mg/kg instillation, the GSH-Px activities in

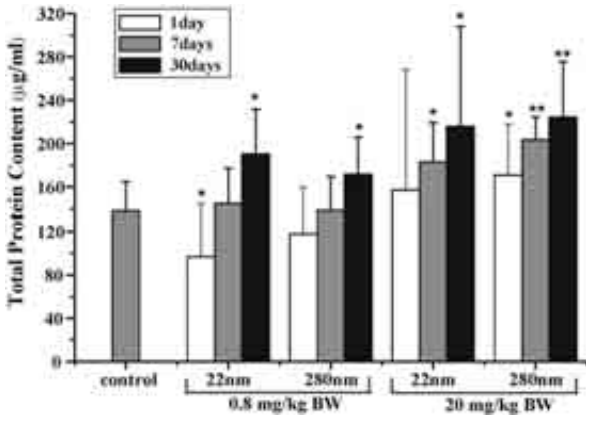

Fig. 2. Levels of total protein in BALF. Values are mean ± S.D.; n = 6/group. *Significant difference from control ($p < 0.05$); **significant difference from control ($p < 0.01$).

Please cite this article in press as: Zhu, M.-T., et al., Comparative study of pulmonary responses to nano- and submicron-sized ferric oxide in rats, Toxicology (2008), doi:10.1016/j.tox.2008.02.011

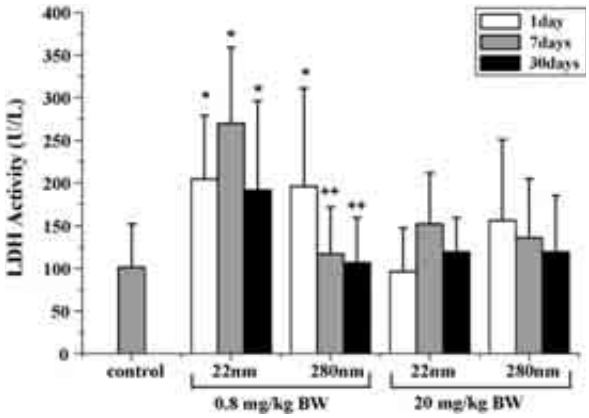

Fig. 3. Levels of LDH in BALF. Values are mean ± S.D.; $n = 6$/group. *Significant difference from control ($p < 0.05$); **significant difference from control ($p < 0.01$); +significant difference between 22 and 280-nm group ($p < 0.05$); ++significant difference between 22 and 280-nm group ($p < 0.01$).

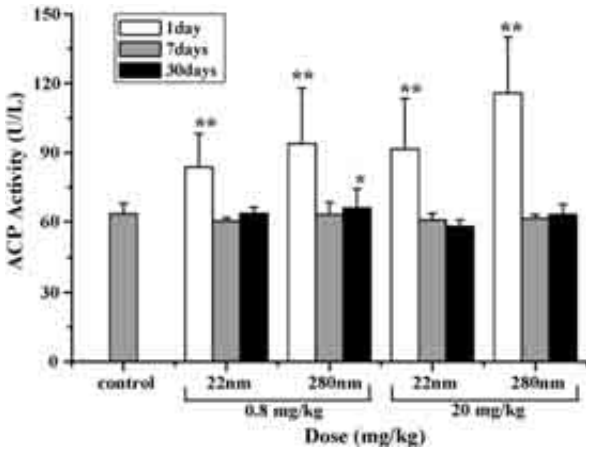

Fig. 4. Levels of ACP in BALF. Values are mean ± S.D.; $n = 6$/group. *Significant difference from control ($p < 0.05$); **significant difference from control ($p < 0.01$).

the 22-nm group rat showed time-dependent increase, while in the 280-nm group rats, the GSH-Px activities increased rapidly at the day 1 post-instillation and then gradually reduced in the following days, which presented different responses in lung between the two-sized Fe_2O_3 particle exposure (Fig. 5).

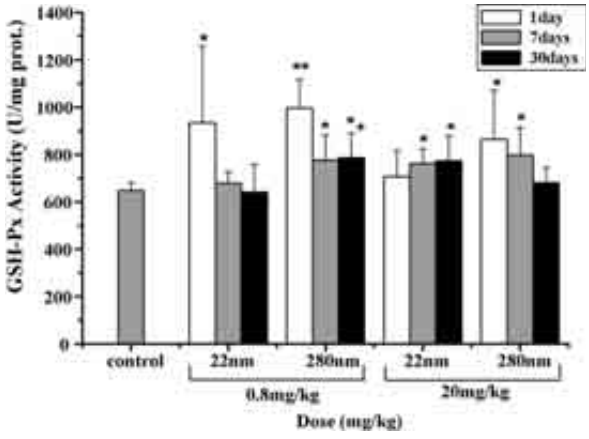

Fig. 5. Activity of GSH-Px in lung homogenates. Values are mean ± S.D.; $n = 6$/group. *Significant difference from control ($p < 0.05$); **significant difference ($p < 0.01$) from control; +significant difference between 22 and 280-nm group ($p < 0.05$).

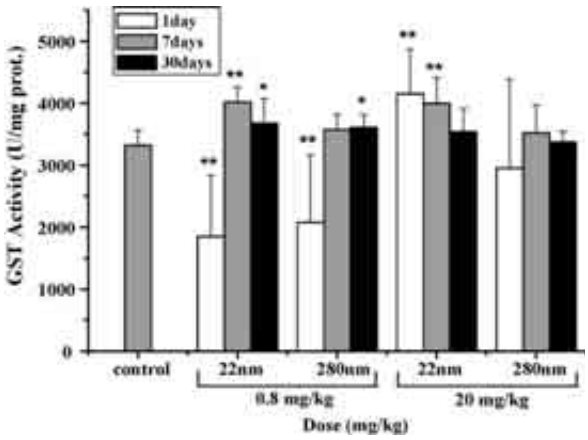

Fig. 6. Activity of GST in lung homogenates. Values are mean ± S.D.; $n = 6$/group. *Significant difference from control ($p < 0.05$); **significant difference from control ($p < 0.01$).

GST activities showed significant decrease in the lung of both the 22 nm- and 280 nm-Fe_2O_3 instilled rats at low dose in day 1 post-instillation, but then significantly increased at post 7 and 30 days. However, in the 22-nm high dose group, GST significantly elevated at post-instilled day 1, then decreased in the subsequent days, whereas, at the same dose of 280-nm group rats, no statistic changes of GST in the time course have been detected (Fig. 6).

The contents of T-GSH decreased in both 22 nm- and 280 nm-Fe_2O_3 instilled rats at 1–7 post-instilled days and then recovered to the control level at the day 30 (Fig. 7). The ratio changes of GSSG/GSH were analyzed at the post-instilled day 7 and 30, which remained around 0.11, indicating no significant changes have occurred.

MDA was measured to estimate lipid peroxidation extent in lung. As shown in Fig. 8, the contents of MDA in 22-nm (20 mg/kg bw) and 280-nm (0.8 and 20 mg/kg bw) group rats presented a time-dependent increase in lung. At the day 30, significant increase of MDA was found in all the particle-treated rats ($p < 0.05$), except for the 22 nm-Fe_2O_3 instilled rats at low dose.

The levels of NO showed significant decrease in lung of the particle-treated rats at the day 1 post-instillation, except for the 280 nm-Fe_2O_3 instilled rat at high dose, then the content of NO gradually elevated with the post-instillation time, at the day 30, NO in all the particle-treated rats recovered to the normal as control (Fig. 9).

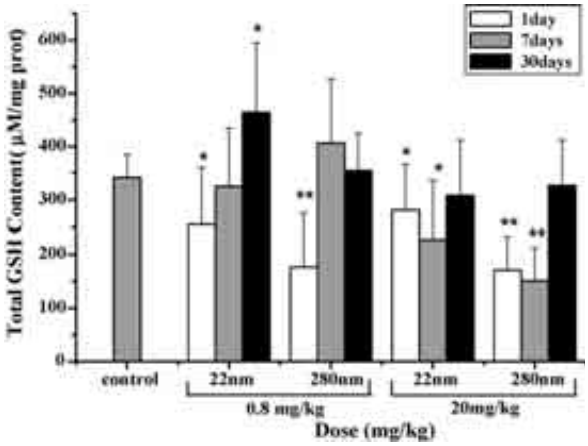

Fig. 7. Contents of GSH in lung homogenates. Values are mean ± S.D.; $n = 6$/group. *Significant difference from control ($p < 0.05$); **significant difference from control ($p < 0.01$).

Please cite this article in press as: Zhu, M.-T., et al., Comparative study of pulmonary responses to nano- and submicron-sized ferric oxide in rats, Toxicology (2008), doi:10.1016/j.tox.2008.02.011

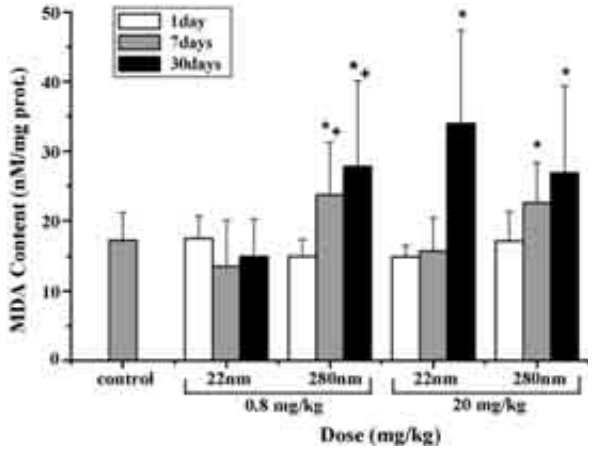

Fig. 8. Contents of MDA in lung homogenates. Values are mean ± S.D.; $n = 6$/group. *Significant difference from control ($p < 0.05$); **significant difference from control ($p < 0.01$); +significant difference from 22-nm group ($p < 0.05$).

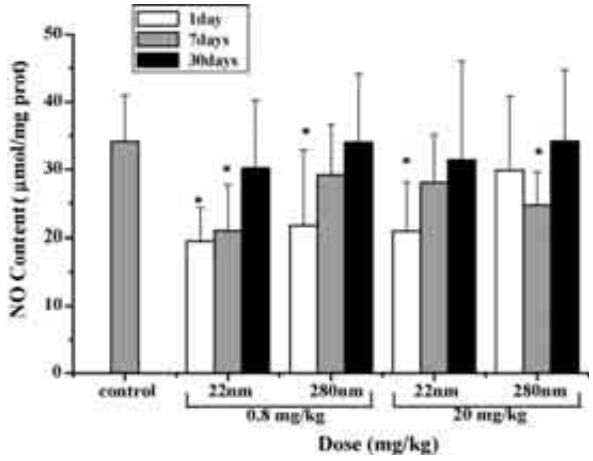

Fig. 9. Contents of NO in lung homogenates. Values are mean ± S.E.M.; $n = 6$/group. *Significant difference from control ($p < 0.05$); **significant difference from control ($p < 0.01$).

3.3. Blood coagulation test

The typical coagulation parameters in blood were observed to estimate the effect of Fe_2O_3 particle intratracheal exposure on animal haemal system. The prolongation of PT and APTT were found in the low and high dose particle-treated rats. At the post-instilled day 30, PT and APTT in low dose of 22 nm-Fe_2O_3 rats were significantly longer than the controls. In the 280 nm-Fe_2O_3 instilled rats, slightly elevated average concentration of FIB was observed (Table 3.).

Table 4
Pathological changes of lung after Fe_2O_3 particle intratracheal instillation

	Post-days	0.8 mg/kg bw		20 mg/kg bw	
		22 nm	280 nm	22 nm	280 nm
Follicular hyperplasia	7	+	+	+++	++
	30	−/+	+	++	+
Capillary hyperaemia	7	+	+/++	++	++
	30	++	++	+++	++
Emphysema	7	++	+/++	+++	+++
	30	+	++	++/+++	++++
Phagocyte effusion	7	+	++	++/+++	+++
	30	−/+	+	++	+

3.4. Histopathology

The pathological changes in lung were evaluated with HE staining in Figs. 10 and 11. The follicular lymphoid hyperplasia with inflammatory cells aggregated around bronchia were observed in both the 22 nm- and the 280 nm-Fe_2O_3 instilled rats from days 7 to 30 post-instillation, and the injury was more severe with the treated dose increase (Figs. 10 and 11). The thickened alveolar walls were found in all the particle-treatment rats, indicating the earlier fibrosis formation (Fig. 10). Particles phagocytosed by macrophage were observed in the pulmonary alveoli (Fig. 11). The iron particles appeared over-loading in alveolar macrophage by the high dose of 20 mg/kg bw instillation (Fig. 11). Inside the pulmonary alveolus, the inflammatory cells, such as neutrophils, lymphocytes and eosinophils could be found (Fig. 12). At the day 30 post-instillation, the inflammatory responses still extended, presenting as the severe follicular hyperplasia of the lymph node, capillary hyperaemia, alveolar lipoproteinosis and emphysema (Figs. 11 and 12). The pathological changes were summarized in Table 4. To summarize, the pathological examination indicates that both the 22 nm- and 280 nm-Fe_2O_3 intratracheal instillation could induce lung injury and the injury would more severe with the treated dose increase.

3.5. TEM inspection

The images of TEM presented the increase of lysosome in the lung. On the post-instilled day 30, mitochondria tumefaction and organelles dissolution indicating the damage of alveolar epitheliums occurred. The increased amount of collagen formation was observed, showing a tendency sign of lung fibrosis induction. In the meantime, particles translocated into the lung epithelium in the days 1 and 7 can be observed as well (Fig. 13).

Table 3
The levels of PT, APPT and FIB in blood

	Post-days	Control	0.8 mg/kg bw		20 mg/kg bw	
			22 nm	280 nm	22 nm	280 nm
PT (s)	7	14.34	14.78 ± 1.13	14.93 ± 0.86	14.64 ± 0.92	15.02 ± 0.63
	30	± 0.90	15.44 ± 0.96*	15.62 ± 0.85*	14.48 ± 0.96	14.73 ± 0.87
APPT (s)	7	17.46	19.88 ± 3.63	18.87 ± 1.77	19.92 ± 1.36*	17.78 ± 1.98
	30	± 1.86	21.13 ± 2.22**	18.00 ± 1.44	19.50 ± 1.63	18.43 ± 4.73
FIB (mg/dL)	7	213.4	213.0 ± 40.5	256.9 ± 40.0	220.7 ± 41.3	248.0 ± 39.4
	30	± 48.5	204.7 ± 29.9	230.5 ± 33.3	197.2 ± 29.6	220.8 ± 45.8

Data represent the mean ± S.D. ($n = 6$/group).
* Significant difference from control, $p < 0.05$.
** Significant difference from control, $p < 0.01$.

Please cite this article in press as: Zhu, M.-T., et al., Comparative study of pulmonary responses to nano- and submicron-sized ferric oxide in rats, Toxicology (2008), doi:10.1016/j.tox.2008.02.011

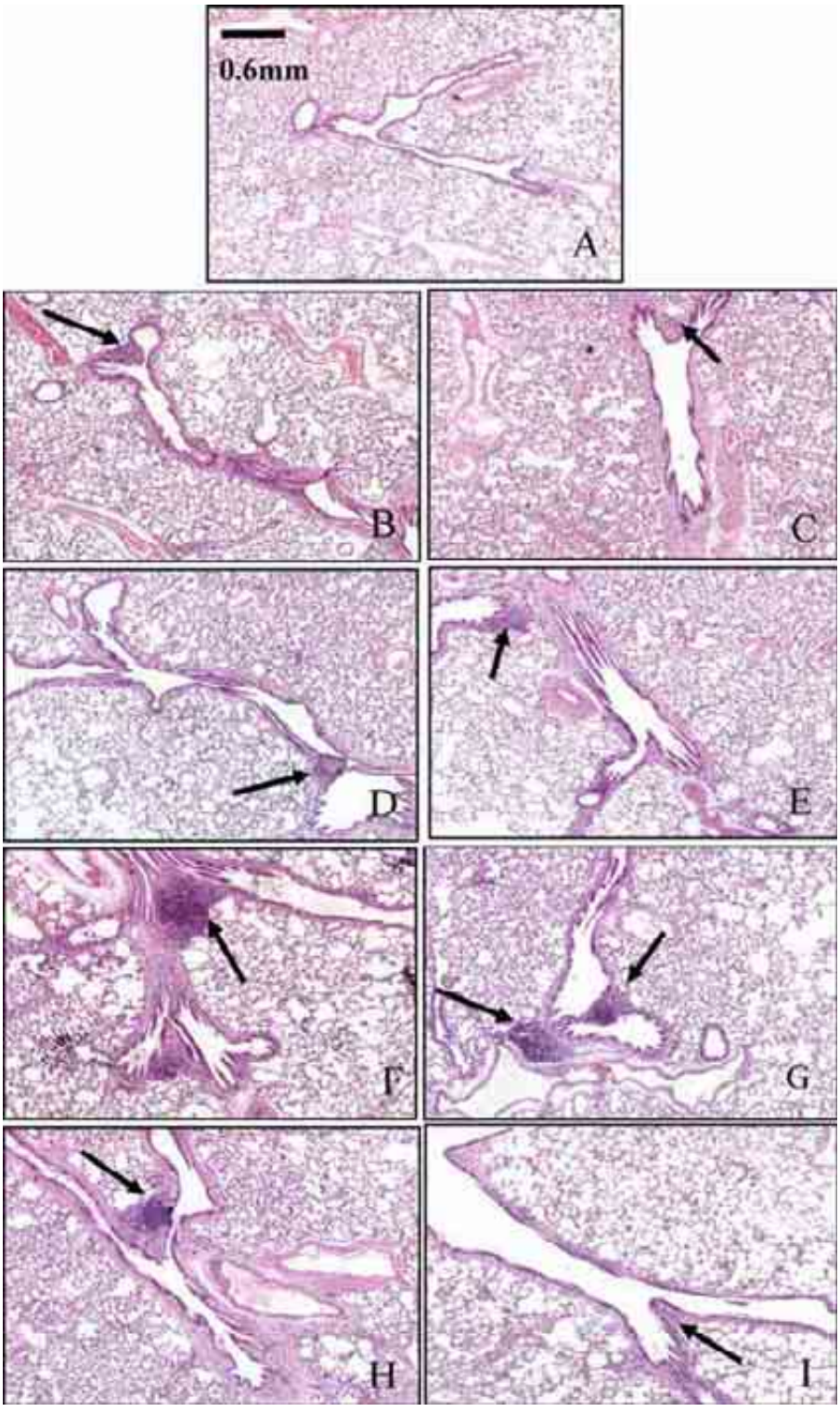

Fig. 10. Histopathology of lung at days 7 and 30 after intratracheal instillation of particles or saline (hematoxylin–eosin stain, magnification = 50). Follicular hyperplasia of the lymph node was formed at trachea forks (dark arrow). (A) Control group; (B) days 7 after instillation of 0.8 mg/kg bw 22 nm-Fe_2O_3; (C) days 30 after instillation of 0.8 mg/kg bw 22 nm-Fe_2O_3; (D) days 7 after instillation of 0.8 mg/kg bw 280 nm-Fe_2O_3; (E) days 30 after instillation of 0.8 mg/kg bw 280 nm-Fe_2O_3; (F) days 7 after instillation of 20 mg/kg bw 22 nm-Fe_2O_3; (G) days 30 after instillation of 20 mg/kg bw 22 nm-Fe_2O_3; (H) days 7 after instillation of 20 mg/kg bw 280 nm-Fe_2O_3; (I) days 30 after instillation of 20 mg/kg bw 280 nm-Fe_2O_3.

4. Discussion

Generally, the oxidative stress caused by the particle is considered to be one of the important mechanisms of nanoparticle toxicity, especially for those particles containing transition metals. Based on increasing experimental results (Simeonova and Luster, 1995; Chao et al., 1996), it is hypothesized that the respiratory and cardiovascular diseases caused by transition metal or its oxide particle exposure may be due to the induction of reactive oxygen species (ROS) and reactive nitrogen species (RNS). We demon-

Please cite this article in press as: Zhu, M.-T., et al., Comparative study of pulmonary responses to nano- and submicron-sized ferric oxide in rats, Toxicology (2008), doi:10.1016/j.tox.2008.02.011

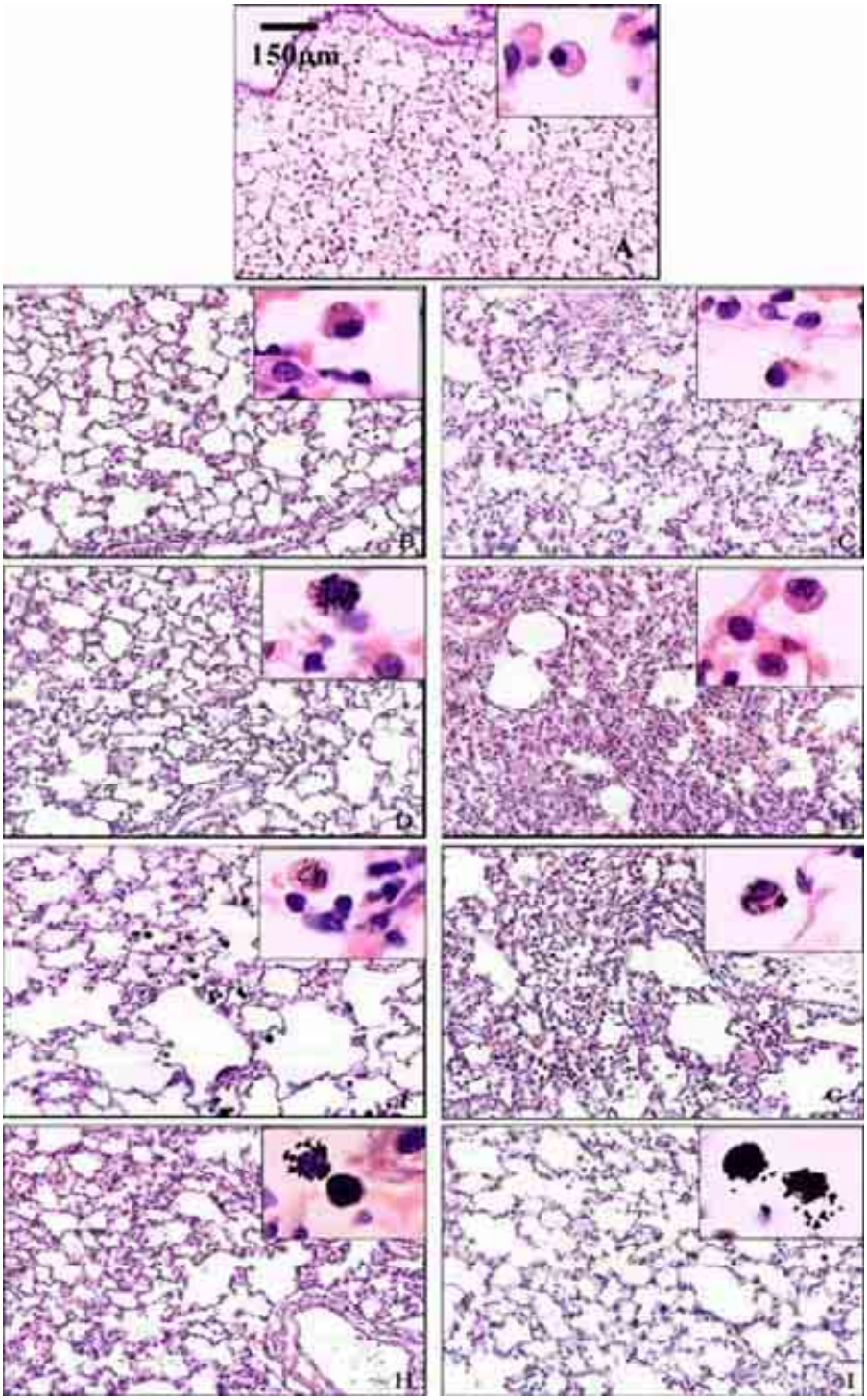

Fig. 11. Histopathology of the lungs at days 7 and 30 after intratracheal instillation of particles or saline (hematoxylin–eosin stain). Phagocytosis of particles by alveolar macrophages was shown on the right-top (magnification = 200). (A) Control group; (B) days 7 after instillation of 0.8 mg/kg bw 22 nm-Fe_2O_3; (C) days 30 after instillation of 0.8 mg/kg bw 22 nm-Fe_2O_3; (D) days 7 after instillation of 0.8 mg/kg bw 280 nm-Fe_2O_3; (E) days 30 after instillation of 0.8 mg/kg bw 280 nm-Fe_2O_3; (F) days 7 after instillation of 20 mg/kg bw 22 nm-Fe_2O_3; (G) days 30 after instillation of 20 mg/kg bw 22 nm-Fe_2O_3; (H) days 7 after instillation of 20 mg/kg bw 280 nm-Fe_2O_3; (I) days 30 after instillation of 20 mg/kg bw 280 nm-Fe_2O_3.

strated that the nano- and submicron-sized Fe_2O_3 particles could generate inflammation and mediate oxidative stress in lung by either low or high dose intratracheal exposure. In our study, T-GSH, GSH-Px and GST were simultaneously measured to evaluate the oxidative stress in lung tissues after ferric oxide particle exposure. Increase of both GSH-Px and GST and decrease of T-GSH levels in Fe_2O_3-particle instilled rat indicated that the antioxidant defense system in lung tissues might over-load. Decrease of NO content in lung tissues after exposure at the first post-instilled day might be explained by free radical reactions. It is known that superfluous ROS may react with NO in the process of producing highly reactive and cytotoxic nitrogen products, such as peroxynitrite (ONOO-) and peroxynitrous acid (ONOOH). Peroxynitrite in turn reacts with and modifies various molecules, such as lipids, DNA, and proteins,

Please cite this article in press as: Zhu, M.-T., et al., Comparative study of pulmonary responses to nano- and submicron-sized ferric oxide in rats, Toxicology (2008), doi:10.1016/j.tox.2008.02.011

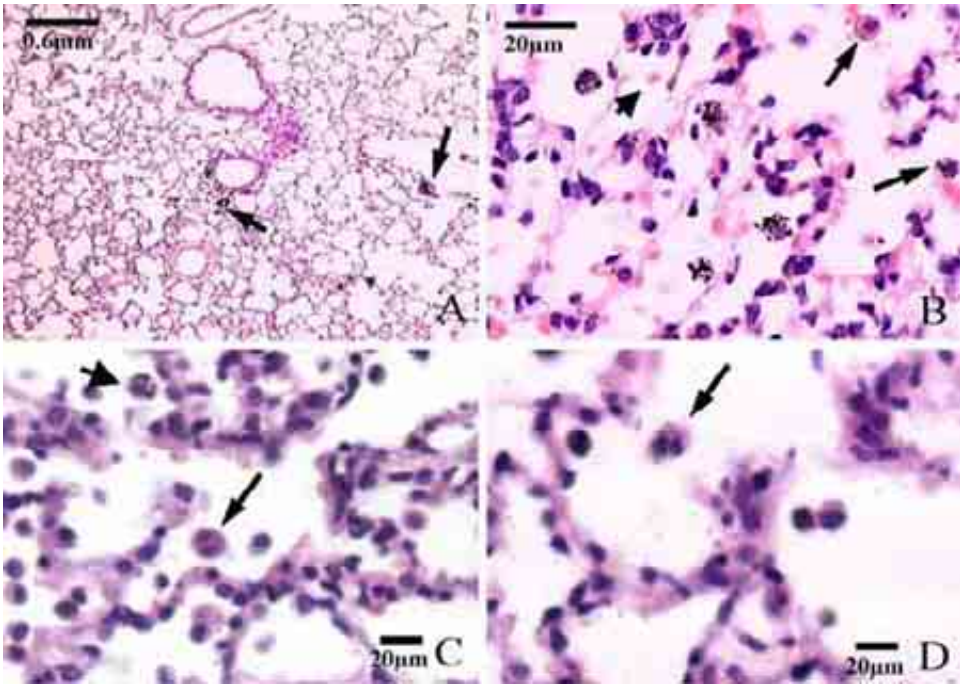

Fig. 12. (A) Phagocytosed alveolar macrophages clustered in alveolus (thin arrow); (B) alveolar lipoproteinosis (thick arrow) and foamy alveolar macrophages were presented; (C) eosinophils egressed (thin arrow) and particle-laden alveolar macrophages (thick arrow); (D) neutrophils margination and egress into alveolar space.

resulting in functional NO deficiency. The significant increase of MDA at post-instillation day 30 demonstrated that lipid peroxidation had occurred. Another possibility of NO decrease might result from the synthesis of NO reduction, which may probably predict the injuries of cell functions.

It is hypothesized that oxidative stress could exert the macrophages on nanoparticles phagocytosis (Donaldson et al., 1998). Nanoparticles were found to deposit in the most distal parts of the lungs and had direct contact with the membrane of airways and alveoli (Brown et al., 2000). Depending on particle size, surface chemistry and possible charge, nanoparticles were reported to across epithelial and endothelial cell layers and translocated into the circulatory system within minutes after inhalation (Mehta et al., 2004; Heckel et al., 2004). We have observed in our pathological and TEM images that particles were phagocytosed by AM and entered alveolar epithelium, which supported the hypothesis that ultrafine particles were hard to be cleared from lungs. Moreover, the above results also suggested that Fe_2O_3 nanoparticle exposure may probably stimulate both the AM and epithelium cells. In the histopathological observation, the activated AMs presented in alveolus as a clustered form (Fig. 12A) and some were in foamy condition (Fig. 12B). The inflammatory cells of neutrophils, lymphocytes and eosinophils were observed as well. The increasing numbers of neutrophils and lymphocytes cells in BALF at days 7 post-instillation demonstrated that the inflammation of lung had occurred. Furthermore, phagocytosis of particles may stimulate AM releasing proinflammatory cytokines such as interleukin 1 (IL-1), interleukin 8 (IL-8), and tumor necrosis factor (TNF), which may activate neutrophils and eosinophils marginating and egressing into alveolar space, as similar results showed in our pathological results (Fig. 12C and D). The activated neutrophils and eosinophils are the rich source of leukotrienes, protease, platelet activating factor (PAF), etc., which contribute to local tissue damage, thus, inflammatory response can be amplified and sustained. In our study, the inflammation of lung has been found from days 7 till 30 of post-instillation (Figs. 12 and 13). In the TEM images, the significant acute inflammatory reaction in lung after irritant exposure of Fe_2O_3 particle has been presented as follicular hyperplasia of the lymph node, protein effusion, pulmonary capillary vessel hyperaemia and alveolar lipoproteinosis (Fig. 13B). Consistently, the increases in microvascular permeability and cell lysis in lung epitheliums were found by the determination of total protein, LDH and ACP activities, suggesting the injury of lung epitheliums after Fe_2O_3 nanoparticle instillation as well. Similar results have been reported by Hetland et al. (2004) that exposure to ultrafine ambient PM induced cell toxicity and apoptosis in lung epithelial cells.

The macrophages over-loaded by the phagocytosis of particles were clearly presented in the lung TEM images of days 7 and 30 post-instillation, though the lysosome increase was shown to resist the particles in the early days, the subsequent alveolar epitheliums damage had still occurred, including mitochondria tumefaction and organelles dissolution. More severely, the alveolar walls thickening and collagen formation in lung epitheliums can be observed, indicating the pro-sign of lung fibrosis induction. Shvedova et al. (2005) reported that pharyngeal aspiration of SWCNTs could lead to fibrosis and granuloma formation. In our study, emphysema that presented as destruction of alveolar walls had formed in the early days after instillation and had changed to exacerbation in latter days, which may be due to the long-term and over-loaded deposition of Fe_2O_3 particles in alveolar. All those pathological changes combined with the biochemical alteration in BALF indicated an acute aspiration pneumonia symptom. Though some biochemical and oxidative stress markers recovered to the control levels in the later time course, however, pathological and TEM observation indicated that the lung injury could sustain for relatively long time even without repeated particle exposure.

The inflammatory reactivities of alveolar macrophages, neutrophils, eosinophils and epithelial cells can generate cytokines and ROS (Donaldson et al., 1998), which may continuously enhance the content of fibrinogen in blood and influence blood coagulation system. It was reported that the ROS induced by transition metal particle could arouse lipid peroxidation *in vivo* and subsequently cause atheromatous plaques or inflammation, which might result in fibrinogen formation and vessel viscosity increase

Please cite this article in press as: Zhu, M.-T., et al., Comparative study of pulmonary responses to nano- and submicron-sized ferric oxide in rats, Toxicology (2008), doi:10.1016/j.tox.2008.02.011

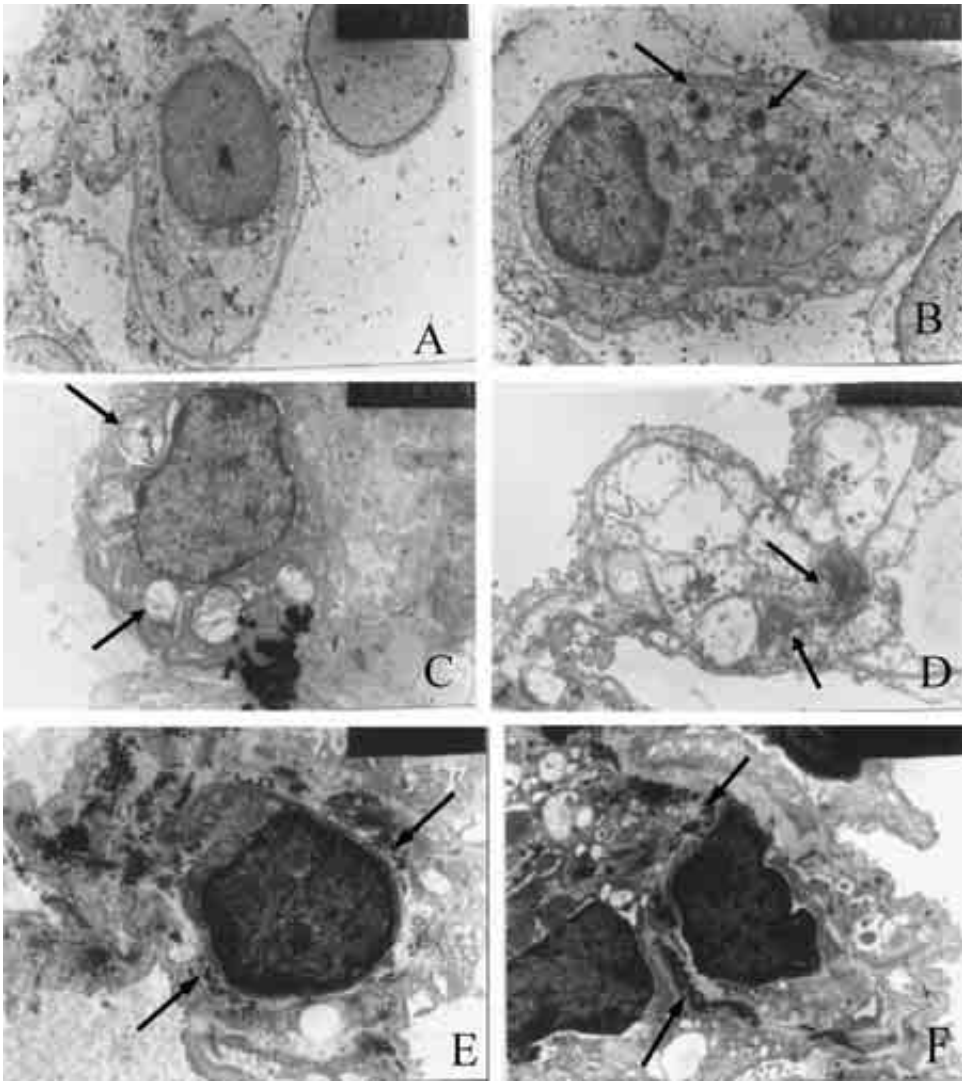

Fig. 13. TEM images of the lungs at days 7 and 30 after intratracheal instillation of particles or saline (magnification = 8000). (A) Control group; (B) days 7 after instillation of 20 mg/kg bw 22 nm-Fe_2O_3. Lysosome increased in lung type II epithelium; (C) and (D) days 30 after instillation of 20 mg/kg bw 280 nm-Fe_2O_3. Mitochondria tumefaction (C) and organelles dissolution (D) (thin arrow) were shown. The increased amount of collagen formation could be observed: (E) 1 day after instillation of 20 mg/kg bw 22 nm-Fe_2O_3. Particles translocated into the lung epitheliums (thin arrow); (F) days 7 after instillation of 20 mg/kg bw 22 nm-Fe_2O_3. Particles translocated into the lung epitheliums (thin arrow).

(Sorensen et al., 2003). In population exposed to air pollution episodes, the levels of blood viscosity, fibrinogen, and C-reactive protein (CRP) were found higher than normal (Seaton et al., 1995; Berry et al., 1977). In this study, though not all of the chemical markers of blood coagulation exhibited significant differences between the particle-treated and control rats, prolongation of PT, APTT and higher level of FIB in Fe_2O_3 particle-treated rats were observed. It is noteworthy that PT and APTT in the low dose of 22 nm-Fe_2O_3 instilled rats were significantly prolonged than in the control, suggesting that the 22 nm-sized particles may be more susceptible to affect coagulation process. Similar observations were found in previous researches as well (Inoue et al., 2006; MacNee and Donaldson, 2000). These previous findings suggested that smaller sized nanoparticles could facilitate coagulatory disturbance because of oxidative stress and inflammation in lung, which induced endothelial-epithelial damage and subsequent infiltrated leukocytes allowed large amounts of smaller nanoparticles to pass easily into circulation (Inoue et al., 2006; MacNee and Donaldson, 2000). Our results supported the previous studies that the prolongation of PT and APTT in 22-nm groups might result from the 22 nm-Fe_2O_3 nanoparticles diffusion in blood circulation and the generation of local and systemic oxidative stress and inflammation.

In conclusion, we demonstrated that both of the nano- and micron-sized Fe_2O_3 particle intratracheal exposure could initiate acute lung injury. Oxidative stress in lung was induced. The phagocytosis of nanoparticle by AMs in lung was over-loaded after high dose exposure. The non-phagocytosed particles were found to enter into alveolar epithelial, suggesting that nanoparticles may be taken up by epithelium cells and hard to be cleared from lungs. The long term and over-loaded of particles in AM and epithelium cells could even cause pathological symptoms of lung emphysema and the pro-sign of lung fibrosis. More attention should be paid on the toxic effect induced by nano-sized Fe_2O_3 particle. Our results suggest that nano-sized Fe_2O_3 particle intratracheal instillation may increase microvascular permeability and cell lysis in lung epitheliums and effect on blood coagulation system.

Acknowledgments

The authors are grateful to the foundations of MOST 973 program (2006CB705605, 2006CB932505 and 2007CB935604), the

Please cite this article in press as: Zhu, M.-T., et al., Comparative study of pulmonary responses to nano- and submicron-sized ferric oxide in rats, Toxicology (2008), doi:10.1016/j.tox.2008.02.011

Chinese Academy of Sciences (KJCX3.SYW.N3) and the National Natural Science Foundation of China (10490181, 20475055, 10675139, and 10525524).

References

Atkinson, R.W., Bremner, S.A., Anderson, H.R., Strachan, D.P., Bland, J.M., de Leon, A.P., 1999. Short-term associations between emergency hospital admissions for respiratory and cardiovascular disease and outdoor air pollution in London. Arch. Environ. Health 54, 398–411.

Berry, J.P., Arnoux, B., Stanislas, G., Galle, P., Chretien, J., 1977. A microanalytic study of particles transport across the alveoli: role of blood platelets. Biomedicine 27, 354–357.

Brown, L.M., Collings, N., Harrison, R.M., Maynard, A.D., Maynard, R.L., 2000. Introduction. In: Brown, L.M. (Ed.), Ultrafine Particles in the Atmosphere, Phil. Trans. R. Soc. Lond. A, vol. 358, pp. 2563–2565.

Chao, C.C., Park, S.H., Ann, E.A., 1996. Participation of nitric oxide and iron in the oxidation of DNA in asbestos-treated human lung epithelial cells. Arch. Biochem. Biophys. 326, 152–157.

Donaldson, K., Li, X.Y., MacNee, W., 1998. Ultrafine (nanometer) particle mediated lung injury. J. Aerosol Sci. 29 (5/6), 553–560.

Gamble, J.F., Lewis, R.J., 1996. Health and respirable particulate (PM10) air pollution: a causal or statistical association? Environ. Health Perspect. 104, 838–850.

Gilmour, P.S., Ziesenis, A., Morrison, E.R., Vickers, M.A., Drost, E.M., Ford, I., Karg, E., Mossa, C., Schroeppel, A., Ferron, G.A., Heyder, J., Greaves, M., MacNee, W., Donaldson, K., 2004. Pulmonary and systemic effects of short-term inhalation exposure to ultrafine carbon black particles. Toxicol. Appl. Pharm. 195, 35–44.

Henderson, R.F., 2005. Use of bronchoalveolar lavage to detect respiratory tract toxicity of inhaled material. Exp. Toxicol. Pathol. 57, 155–159.

Hanes, J., Cleland, J.L., Langer, R., 1997. New advances in microsphere-based single-dose vaccines. Adv. Drug Deliv. Rev. 28, 97–119.

Heckel, K., Kiefmann, R., Dorger, M., Stoeckelhuber, M., Goetz, A.E., 2004. Colloidal gold particles as a new in vivomarker of early acute lung injury. Am. J. Physiol. Lung Cell. Mol. Physiol. 287, L867–L878.

Hetland, R.B., Cassee, F.R., Refsnes, M., Schwarze, P.E., Lag, M., Boere, A.J.F., Dybing, E., 2004. Release of inflammatory cytokines, cell toxicity and apoptosis in epithelial lung cells after exposure to ambient air particles of different size fractions. In Vitro Toxicol. 18, 203–212.

Hoet, P.H., Bruske-Hohlfeld, I., Salata, O.W., 2004. Nanoparticles' known and unknown health risks. J. Nanobiotechnol. 2, 12–27.

Hood, E., 2004. Nanotechnology: looking as we leap. Environ. Health Perspect. 112 (13), A740–A749.

Hubbell, J.A., Langer, R., 1995. Tissue engineering. Chem. Eng. News, 42–54 (March 13).

Hughes, L.S., Cass, G.R., Gone, J., Ames, M., Olmez, I., 1998. Physical and chemical characterization of atmospheric ultrafine particles in the Los Angeles area. Environ. Sci. Technol. 32, 1153–1161.

Inoue, K., Takano, H., Yanagisawa, R., Hirano, S., Sakurai, M., Shimada, A., Yoshikawa, T., 2006. Effects of airway exposure to nanoparticles on lung inflammation induced by bacterial endotoxin in mice. Environ. Health Perspect. 114 (9), 1325–1330.

Lam, C.W., James, J.T., McCluskey, R., Hunter, R.L., 2004. Pulmonary toxicity of single-wall carbon nanotubes in mice 7 and 90 days after intratracheal instillation. Toxicol. Sci. 77, 126–134.

Limbach, L.K., Wick, P., Manser, P., Grass, R.N., Bruinink, A., Stark, W.J., 2007. Exposure of engineered nanoparticles to human lung epithelial cells: influence of chemical composition and catalytic activity on oxidative stress. Environ. Sci. Technol. 41 (11), 4158–4163.

MacNee, W., Donaldson, K., 2000. How can ultrafine particles be responsible for increased mortality? Monaldi Arch. Chest Dis. 55 (2), 135–139.

Mehta, D., Bhattacharya, J., Matthay, M.A., Malik, A.B., 2004. Integrated control of lung fluid balance. Am. J. Physiol. Lung Cell. Mol. Physiol. 287, L1081–L1090.

Oberdörster, G., Oberdörster, E., Oberdörster, J., 2005. Nanotoxicology: an emerging discipline evolving from studies of ultrafine particles. Environ. Health Perspect. 113, 823–839.

Pope III, C.A., Dockery, D.W., Schwartz, J., 1995. Review of epidemiological evidence of health effects of particulate air pollution. Inhal. Toxicol. 7, 1–18.

Renwick, L.C., Donaldson, K., Clouter, A., 2001. Impairment of alveolar macrophage phagocytosis by ultrafine particles. Toxicol. Appl. Pharmacol. 172, 119–127.

Shvedova, A.A., Kisin, E.R., Mercer, R., Murray, A.R., Johnson, V.J., Potapovich, A.I., Tyurina, Y.Y., Gorelik, O., Arepalli, S., Schwegler-Berry, D., Hubbs, A.F., Antonini, J., Evans, D.E., Ku, B.K., Ramsey, D., Maynard, A., Kagan, V.E., Castranova, V., Baron, P., 2005. Unusual inflammatory and fibrogenic pulmonary responses to single-walled carbon nanotubes in mice. Am. J. Physiol. Lung Cell. Mol. Physiol. 289, L698–L708.

Seaton, A., MacNee, W., Donaldson, K., Godden, D., 1995. Particulate air pollution and acute health effects. Lancet 345, 176–178.

Simeonova, P.P., Luster, M.I., 1995. Iron and reactive oxygen species in the asbestos-induced tumor necrosis factor-alpha response from alveolar macrophages. Am. J. Respir. Cell. Mol. Biol. 12 (6), 676–683.

Sorensen, M., Autrup, H., Moller, P., et al., 2003. Linking exposure to environmental pollutants with biological effects. Mutat. Res. 544, 255–271.

Torres-Martínez, C.L., Kho, R., Mian, O.I., Mehra, R.K., 2001. Efficient photocatalytic degradation of environmental pollutants with mass-produced ZnS nanocrystals. J. Colloid Interface Sci. 240, 525–532.

Xu, H., Vanhooren, H., Verbeken, E., Nemery, B., Hoet, P.H.M., 2003. Pulmonary toxicity of polyvinyl chloride particles after a single intratracheal instillation in rats. Time course and comparison with silica. Toxicol. Appl. Pharmacol. 194, 111–121.

Zhou, Y.M., Zhong, C.Y., Ian, M.K., Kent, E.P., 2003. Pinkerton pulmonary responses of acute exposure to ultrafine iron particles in healthy adult rats. Environ. Toxicol. 18, 227–235.

Please cite this article in press as: Zhu, M.-T., et al., Comparative study of pulmonary responses to nano- and submicron-sized ferric oxide in rats, Toxicology (2008), doi:10.1016/j.tox.2008.02.011